Lanthanide-Induced Peptide Folding: Variations in Lanthanide Affinity and Induced Peptide Conformation†

Jean Gariépy, Brian D. Sykes, and Robert S. Hodges*

ABSTRACT: The present work has demonstrated the utility of the diamagnetic lanthanides lutetium and lanthanum as metal binding probes for a synthetic 13-residue fragment representing calcium binding site 3 of rabbit skeletal troponin C (residues 103–115). The peptide conformation induced by these metals was monitored by the proton magnetic resonance at 270 MHz. The peptide affinity for these rare earths is 50–400 times higher than that for calcium ($K_{Lu^{3+}}$, 1.3×10^4 M^{-1}; $K_{La^{3+}}$, 1.1×10^5 M^{-1}; $K_{Ca^{2+}}$, 3×10^2 M^{-1}) which is related to the change in cation charge from 2+ to 3+. The peptide conformation induced by the presence of La^{3+} generates a different ^1H NMR spectrum than the one observed for the lutetium-saturated peptide. Thus, it appears that these metals do not fold the peptide into exactly the same conformation. The resonance shifts observed during the Lu^{3+} titration are much smaller than those seen in the case of La^{3+} addition. The fact that lutetium binds less tightly than lanthanum to the peptide may be linked directly or indirectly to the difference in ionic radius between these metals (Lu^{3+}, 0.86 Å; La^{3+}, 1.03 Å). This may in turn indicate that the peptide primary sequence encodes for some aspects of metal ion specificity. The ^1H NMR results also demonstrate that glycine-108 adopts a restricted geometry in the absence of metal such that its two α-carbon protons are in different environments which are further affected by the addition of either metal. These observations support the concept that geometric constraints arising from the particular peptide folding pattern near this residue correlate with the highly conserved nature of this site of the EF hand. This position remains occupied by glycine in most EF hand domains with the exception of known distorted calcium binding sites present in intestine calcium binding proteins and S-100 [Szebenyi, D. M. E., Obendorf, S. K., & Moffat, K. (1981) *Nature (London) 294*, 327–332].

Calcium acts as a cytosolic second messenger by virtue of its interaction with as many as 70 different proteins (Kretsinger, 1976). A particular class of calcium binding proteins are homologous to one another and contain EF hand[1] domains (Kretsinger & Nockolds, 1973). Because of the affinity and specificity of these domains for calcium, Kretsinger (1977, 1979) postulated that the calcium modulation of cellular events occurs through the action of proteins containing EF hands. This class includes proteins such as troponin C, calmodulin, and parvalbumin.

An understanding of the EF sites was partially achieved by the examination of the two calcium binding sites present in the crystal structure of carp parvalbumin (Kretsinger & Nockolds, 1973) and by the primary sequence alignment of related proteins (Barker et al., 1978; Vogt et al., 1979; Kretsinger, 1979, 1980; Reid & Hodges, 1980). However, questions relating to the dynamics of calcium binding and to biochemical events induced by protein folding around the metal remain unanswered. The use of spectroscopic tools such as nuclear magnetic resonance, circular dichroism, and fluorescence has permitted the observation of secondary and tertiary structure perturbations resulting from the binding of calcium to troponin C (Burtnick et al., 1975; Seamon et al., 1977; Levine et al., 1977; Leavis & Kraft, 1978; Hincke et al., 1978, 1981a,b; Nagy & Gergely, 1979; Mrakovcic et al., 1979) and calmodulin (Klee, 1977; Wolff et al., 1977; Walsh et al., 1978, 1979; Seamon, 1979, 1980; Crouch & Klee, 1980; LaPorte et al., 1980) for example. A further analysis of regional effects was achieved by the use of protein fragments containing one or more EF hands. Chemical and enzymatic fragments of troponin C (Leavis et al., 1978; Nagy et al., 1978; Birnbaum & Sykes, 1978; Lee et al., 1979; Evans et al., 1980; Grabarek et al., 1981) have been studied extensively, but the size and choice of such fragments often limit their usefulness in generating information about metal-induced folding and the formation and location of α-helical regions.

A unique approach to the study of metal ion binding is the chemical synthesis of a single metal ion binding site, and analogues thereof, and the comparison of their metal ion binding characteristics (Reid et al., 1980). Synthetic peptides of site 3 of rabbit skeletal troponin C of varying lengths (Reid et al., 1980, 1981; Gariépy et al., 1982) have been used to prove the concerted formation of the N-terminal helical region upon calcium binding to the EF loop. Also, the calcium binding affinity of the site was shown to be dependent on both the presence of C- and N-terminal regions (Gariépy et al., 1982). Metal binding to synthetic analogues of site 2 of rabbit skeletal troponin C has been studied by fluorescence spectroscopy (Kanellis et al., 1983) and ^1H NMR spectroscopy (Lenkinski et al., 1983).

The lanthanides, because of their spectroscopic properties, have been used as calcium analogues to probe the metal binding environment of calcium binding proteins. Reviews by

† From the Department of Biochemistry and the Medical Research Council of Canada Group in Protein Structure and Function, University of Alberta, Edmonton, Alberta, Canada T6G 2H7. *Received November 5, 1982.* This investigation was supported by research grants from the Medical Research Council of Canada, AHFMR and MRC studentships (J.G.), and a research allowance (J.G.) from the Alberta Heritage Foundation for Medical Research.

[1] Abbreviations: AcSTnC(103–115)amide, synthetic N-terminal acetylated rabbit skeletal troponin C fragment, residues 103–115, with a C-terminal amide; CaM, calmodulin; CIDNP, chemically induced dynamic nuclear polarization; CD, circular dichroism; DSS, sodium 4,4-dimethyl-4-silapentane-1-sulfonate; EDTA, ethylenediaminetetraacetic acid; EF hand, Kretsinger's abbreviation of the second calcium binding domain of carp parvalbumin (this site is thought to represent a typical calcium binding domain); FID, free induction decay; HPLC, high-pressure liquid chromatography; i.d., internal diameter; La^{3+}, lanthanum; Lu^{3+}, lutetium; ^1H NMR, proton nuclear magnetic resonance; TnC, calcium binding unit of skeletal muscle troponin; TFA, trifluoroacetic acid.

0006-2960/83/0422-1765$01.50/0

Nieboer (1975), Reuben (1977), and Martin & Richardson (1979) summarize the biological applications of such metals. For example, in the case of carp parvalbumin (Lee & Sykes, 1980a,b, 1981, 1982), the presence of the paramagnetic lanthanide Yb^{3+} induces considerable shifting and broadening of resonances from protons in proximity to the metal. From the analysis of the metal-induced changes in the NMR spectrum, information about the structure of the metal binding site could be obtained.

A crucial property of lanthanides is their strong binding to small synthetic peptides as compared to calcium (Lenkinski et al., 1983; this work). This fact has enabled us to reduce the size of our fragment to only the metal binding region (13 amino acids). We report here the ^1H NMR analysis of a synthetic peptide representing segment 103–115 of rabbit skeletal troponin C site 3 and its interaction with the diamagnetic lanthanide metals lanthanum and lutetium.

Experimental Procedures

Materials. Protected amino acid derivatives and other reagents used for the synthesis were described elsewhere (Reid et al., 1981). Lanthanum chloride and lutetium oxide were obtained from Alfa Inorganics-Ventron (Beverly, MA).

Preparation of AcSTnC(103–115)amide. The peptide was synthesized by stepwise solid-phase peptide synthesis on a Beckman 990 peptide synthesizer. The amino acid protection strategy and the peptide cleavage approach were as previously described (Reid et al., 1981). As in the case of previous analogues of this calcium binding site, the peptide's N terminal was acetylated while the use of a benzhydrylamine resin support generated a C-terminal amide. The elimination of charges at both ends of this fragment appeared appropriate in view of the fact that such charges are not present in the native protein.

The crude peptide was intially purified by high-pressure liquid chromatography (HPLC) on a SynChropak AX300 ion-exchange column (Linden, IN; 250 × 10.0 mm i.d.). The crude peptide was dissolved in 5 mM KH_2PO_4, pH 7.5, buffer, and the sample pH was readjusted to 7.5 with 1 M KOH. The undissolved material was centrifuged. Aliquots of the supernatant were then injected on the column. A gradient was constructed by using 5 mM (buffer A) and 300 mM (buffer B) KH_2PO_4 buffers adjusted to pH 7.5. The program used to isolate the pure peptide was as follows: 100% A, 5 min; linear gradient from 100% A to 85% A: 15% B, 40 min; 85% A: 15% B, 5 min; linear gradient from 85% A: 15% B to 75% A: 25% B, 5 min; linear gradient from 75% A: 25% B to 100% A, 5 min; 100% A, 10 min. The flow rate was 2 mL/min, and the absorbance was recorded at 220 nm by using a 3-mm path cell. Figure 1A illustrated a typical purification pattern observed by using our HPLC approach. The major peak was desalted on an HPLC preparative C-18 SynChropak RP-P column (Linden, IN; 250 × 10.0 mm i.d.). The peptide was dissolved in 0.1% TFA/water, and the pH was adjusted to pH 2.5 with concentrated hydrochloric acid. The peptide was eluted off as a single peak by using a 0–30% gradient of 0.1% TFA/acetonitrile (45-min gradient; 2 mL/min flow rate) (Figure 1B). The composition and concentration of the pure peptide were verified by amino acid analysis (Table I).

Preparation of ^1H NMR Samples. The metal-free spectrum was obtained with an 8.3 mM peptide sample (400 μL) dissolved in 15 mM deuterated imidazole, 100 mM KCl, and 0.2 mM DSS, pH 7.0. The lanthanum and lutetium titrations were performed on 0.8 mM samples of AcSTnC(103–115)-amide taken up in 100 mM KCl/0.1 mM DSS and readjusted to pH 6.0 with a 0.5 N NaOD solution. The pHs of the samples were monitored before and after the metal titration and were shown to remain at their initial value of 6.0. The exact peptide concentrations were determined by amino acid analysis. Alternatively, absorbance measurements at 280 nm (extinction coefficient value of 2100 M^{-1} cm^{-1}) can be used to estimate the peptide concentration.

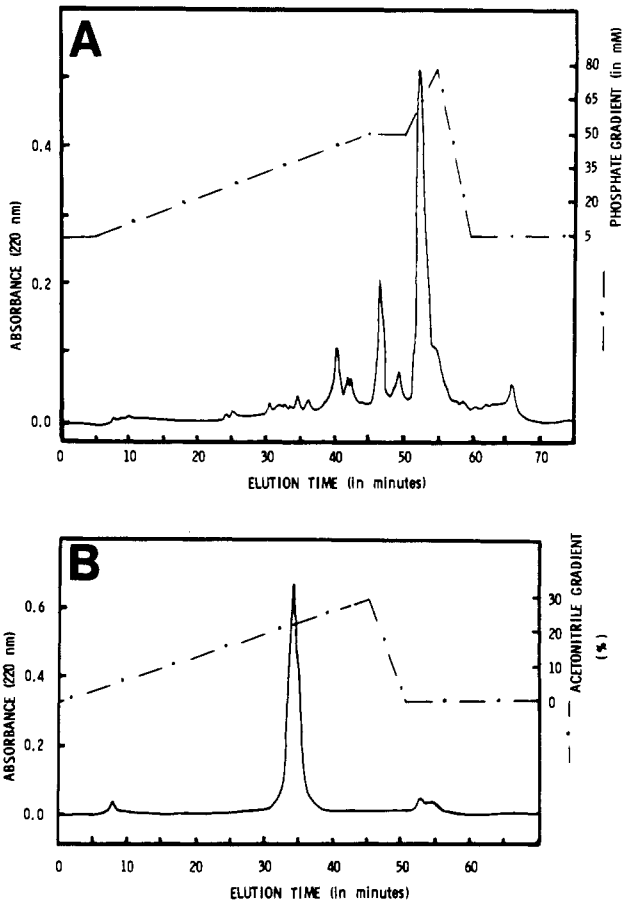

FIGURE 1: Purification strategy of AcSTnC(103–115)amide by high-pressure liquid chromatography. (A) HPLC purification of the crude peptide on a preparative ion-exchange column. The flow rate was 2 mL/min, and 500 μL of a 16 mg/mL solution of the crude peptide was typically injected on the column. The phosphate gradient used to elute the fragment was described under Experimental Procedures. (B) HPLC purification of the major peak eluted from the ion-exchange column on a preparative reverse phase column. The flow rate was 2 mL/min. The 0.1% TFA/water:0.1% TFA/acetonitrile gradient used was described under Experimental Procedures.

Table I: Amino Acid Composition of AcSTnC(103–115)amide

amino acid	observed	sequence[a]
Asx	3.97	4
Glu	2.01	2
Gly	1.02	1
Ala	2.01	2
Ile	0.95	1
Leu	1.02	1
Tyr	0.99	1
Arg	1.04	1

[a] The sequence values are based on the primary sequence of rabbit skeletal troponin C (Collins et al., 1977).

Proton NMR Experiments. Proton NMR experiments were performed on a Bruker HXS 270 MHz spectrometer operating in a Fourier-transform mode and equipped for quadrature detection. For the apopeptide (metal free), the spectrum was obtained from 4000 acquisitions with a sweep width of ±2000 Hz and a 2-s acquisition time. The resolution in the spectrum was enhanced by zero filling the 16K FID to 32K. The de-

Rabbit Skeletal Troponin C Site 3 - Synthetic fragment of the Ca++ binding region

```
      103   105   107   109   111       114
Acetyl-Asp-Arg-Asn-Ala-Asp-Gly-Tyr-Ile-Asp-Ala-Glu-Glu-Leu-NH2
        X     Y     Z    -Y    -X        -Z
```

FIGURE 2: Primary sequence of the synthetic fragment AcSTnC-(103–115)amide. The letters X, Y, Z, –Y, –X, and –Z represent the calcium-coordinating ligands of the peptide.

coupling experiments were performed by irradiating selected resonances in the apopeptide spectrum and observing their connectivities with other resonances. Typically, 256 acquisitions were taken for each spectrum with a sweep width of ±2000 Hz, a 1-s acquisition time, an 8-μs pulse width (~80°), and a line broadening of 1 Hz. Spectrum parameters for the lanthanide titrations where as follows: 4000 acquisitions with a sweep width of ±2000 Hz, a 0.5-s acquisition time, a pulse width of 8 μs, and a spectral line broadening value of 1 Hz.

Metal Ion Analysis. The lanthanum and lutetium solutions used in this study were prepared from reagent-grade $LuCl_3 \cdot 5H_2O$ and Lu_2O_3. The lutetium oxide was converted to its chloride form by addition of an equimolar quantity of hydrochloric acid. The solutions were made up in 100 mM KCl/0.1 mM DSS and adjusted to pH 6.0 with NaOD or DCl. The lanthanum or lutetium content of the solutions was determined by EDTA titration using xylenol orange as the end-point indicator (Lee & Sykes, 1980a).

Calculation of Lanthanide Binding Constants. The following equation was used to determine the quantity Y:

$$Y = (\delta_0 - \delta_F)/(\delta_S - \delta_F)$$

where δ_S represents the chemical shift of a peptide resonance in the metal-saturated spectrum, δ_0 is the observed chemical-shift value for this resonance at a particular point of the titration, and δ_F represents the resonance position in the absence of metal. This quantity was calculated for a variety of resonances during the course of a lanthanide titration. The averaged Y value for each titration point was plotted against the metal:peptide ratio, and the binding constant was determined by a least-squares fitting of the data set to

$$Y = \{(M_0 + P_0 + K_D) - [(M_0 + P_0 + K_D)^2 - 4M_0P_0]^{1/2}\}/2P_0$$

where M_0 and P_0 represent the total concentration of metal and peptide in the sample, respectively, and K_D is the metal dissociation constant to be determined. Note that metal precipitation problems occurred when the peptide solutions were titrated rapidly (addition of large aliquots of metal ion) or when the pH of the peptide solution was close to 7.0 (slow formation of hydroxides). Binding constants were determined from titrations where no precipitation was observed.

Results

Assignments of Apo-AcSTnC(103–115)amide Resonances. The peptide AcSTnC(103–115)amide sequence is presented in Figure 2. One should note the presence of two alanines, three aspartic acids, and two glutamic acids in the sequence as this factor will influence the complexity of the observed ^1H NMR spectrum.

The apopeptide spectrum is shown in Figure 3. The initial assignment of resonances was aided by the published list of proton NMR resonance positions recorded for synthetic peptides containing each amino acid (Bundi & Wurthrich, 1979) and by a spectral record of all the free amino acids at 270 MHz (this work). The integration and decoupling of all the spectral lines permitted the assignment of all spectral regions. However, some regions remain complex because of the sequence composition. Table II lists all the assignments made.

An important assignment is that of the quartet pattern centered at 3.90 ppm to the Gly-108 α-carbon protons. In the spectrum of the free amino acid, the α-carbon protons of glycine are magnetically equivalent and yield a singlet. For the peptide, however, these protons are not equivalent as indicated by the AB pattern in the spectrum. This is in agreement with the spectrum observed for the internal glycine of the synthetic tetrapeptide H-Gly-Gly-Tyr-Ala-OH (Bundi & Wurthrich, 1979). These α-protons also behaved as an AB spin system but were located around 4 ppm ($|\delta_A - \delta_B| = 0.016$ ppm). Bundi and Wurthrich commented that nonrandom spatial arrangements of the amino acid side chains arise from intramolecular short-range interactions independent of the peptide length. In our peptide, the $|\delta_A - \delta_B|$ value is much larger (0.109 ppm) and might be attributed to a further selective orientation of these protons near the ring of tyrosine-109. In the metal-free form, this peptide sequence possesses little secondary structure as observed from CD analysis in the presence and absence of 8 M urea (Reid et al., 1981). A similar conclusion can be drawn from the appearance of a single resonance at 1.4 ppm for the two alanine methyl groups.

Lanthanide Titrations. Lanthanum and lutetium were used in this study because both of them are diamagnetic ($4f^0$ and $4f^{14}$). When these metals are used, no shifting or broadening

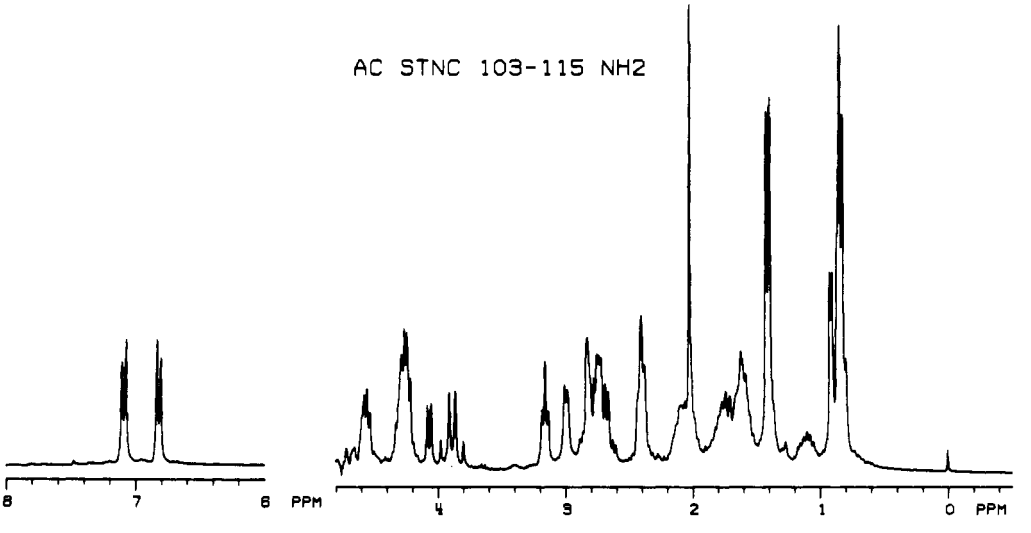

FIGURE 3: ^1H NMR spectrum of apo-AcSTnC(103–115)amide. [Peptide] = 8.3 mM in 15 mM deuterated imidazole, 100 mM KCl, and 0.2 mM DSS, pH 7.0.

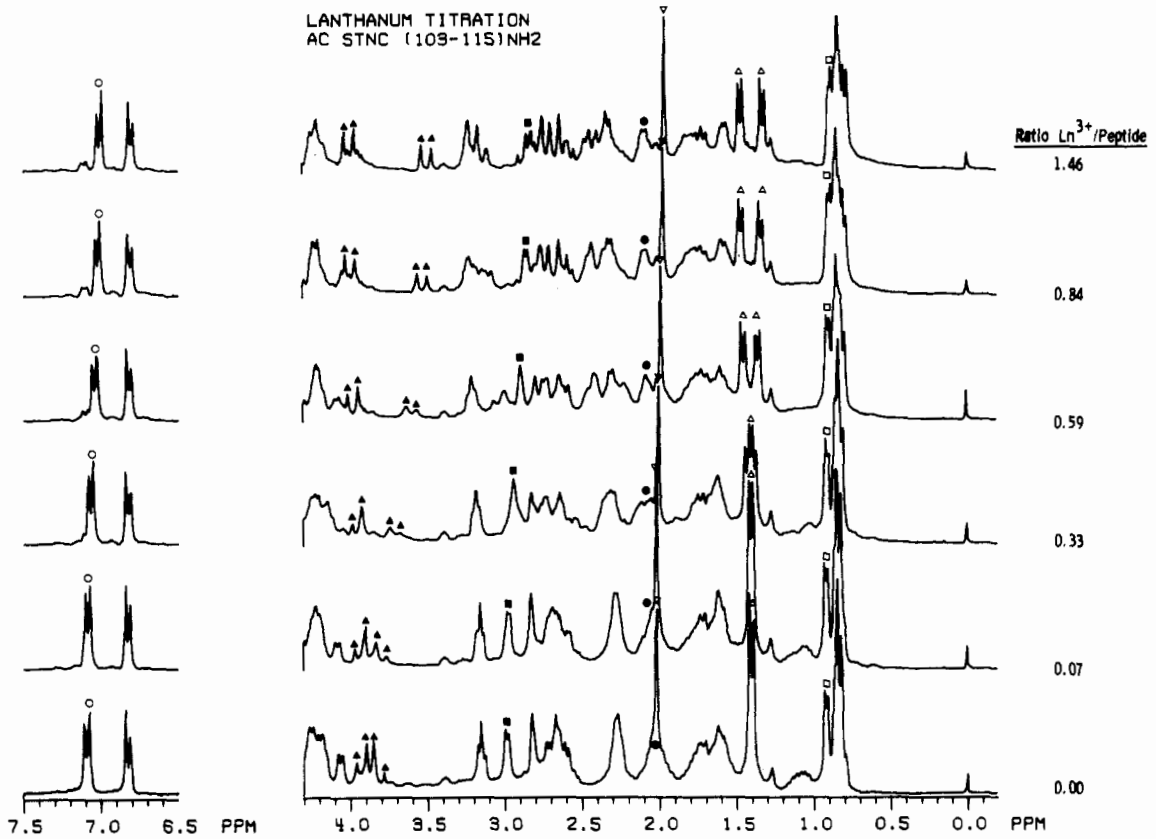

FIGURE 4: Lanthanum titration of AcSTnC(103–115)amide. [Peptide] = 0.8 mM in 100 mM KCl and 0.1 mM DSS, pH 6.0. Symbols highlight changes in the ^{1}H NMR spectrum. The titration was carried out beyond a metal to peptide ratio of 4.

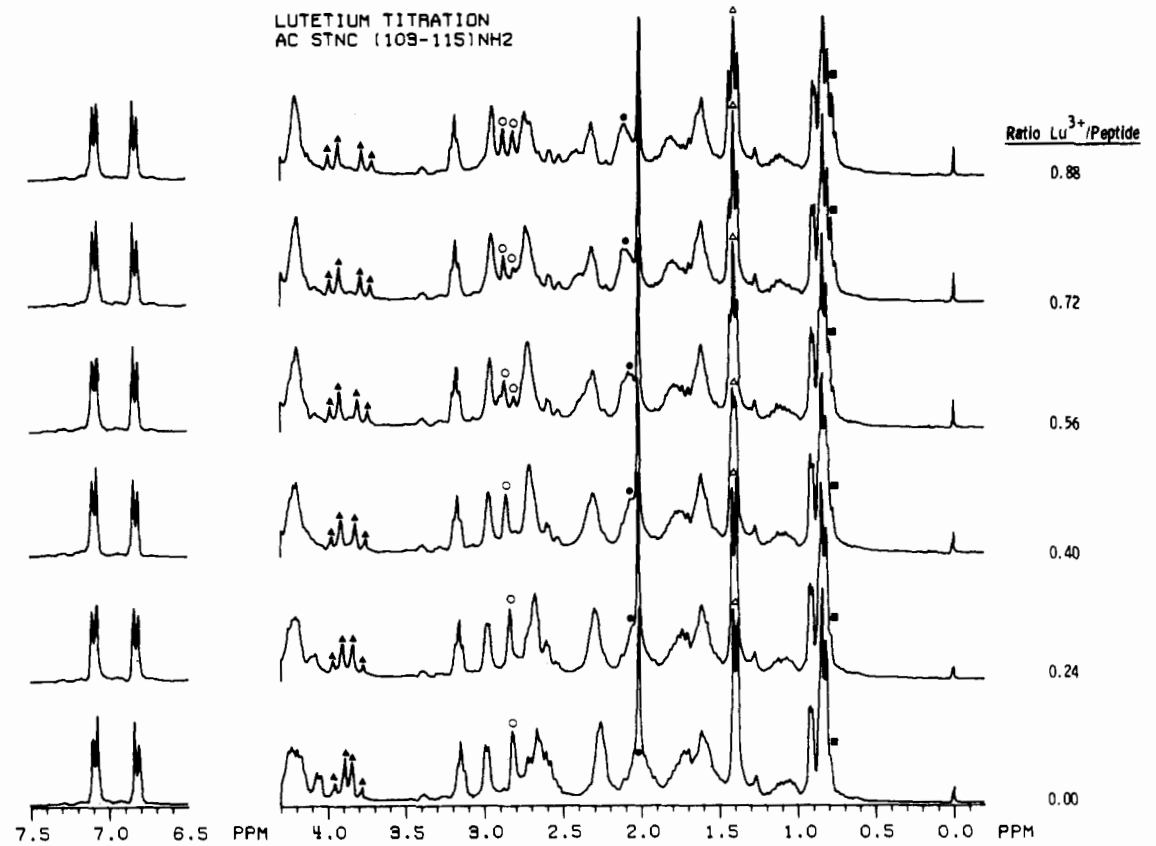

FIGURE 5: Lutetium titration of AcSTnC(103–115)amide. [Peptide] = 0.8 mM in 100 mM KCl and 0.1 mM DSS, pH 6.0. Symbols highlight changes in the ^{1}H NMR spectrum. The titration was carried out beyond a metal to peptide ratio of 4.

of resonances is expected to result from the presence of unpaired electrons on the metal ion. The observed perturbations on the peptide ^{1}H NMR spectrum are the result of a particular geometry adopted by the peptide around these metals. Another advantage in using these two lanthanides is their difference in ionic radius (Lu^{3+}, 0.86 Å; La^{3+}, 1.03 Å; Ca^{2+}, 1.00 Å;

Table II: Assignment of Proton Magnetic Resonances of Apo-AcSTnC(103–115)amide

resonance position (ppm)	resonance pattern observed	proton assignment
0.76–0.87	uneven doublet	ϵ- and δ-CH_3, Leu-115 δ-CH_3, Ile-110
0.88–0.94	doublet	γ-CH_3, Ile-110
1.00–1.20	complex multiplet	γ-CH_2, Ile-110
1.36–1.44	doublet	β-CH_3, Ala-106, -112
1.55–1.65	broad asymmetric peak	γ-CH_2, Arg-104 β-CH, Ile-110 β-CH_2, Leu-115
1.67–1.85	complex multiplet	β-CH_2, Arg-104 γ-CH, Leu-115
2.00	singlet	N-terminal acetyl group, Asp-103
1.95–2.20	broad peak	β-CH_2, Glu-113, -114
2.35–2.45	asymmetric peak	γ-CH_2, Glu-113, -114
2.55–2.90	broad asymmetric multiplet	β-CH_2, Asp-103, -107, -111 β-CH_2, Asn-105
2.95–3.05	doublet	β-CH_2, Tyr-109
3.10–3.22	triplet	δ-CH_2, Arg-104
3.80–4.00	quartet	α-CH_2, Gly-108
4.03–4.10	doublet	α-CH, Ile-110
4.15–4.38	broad multiplet	α-CH, Glu-113, -114 α-CH, Ala-106, -112 α-CH, Arg-104
6.82–6.85	doublet	ring, aromatic 3, 5, Tyr-109
7.08–7.11	doublet	ring, aromatic 2, 6, Tyr-109

Shannon, 1976). By looking at the lanthanum (Figure 4) and lutetium (Figure 5) titrations of the peptide using ^{1}H NMR, it is observed that each metal alters the peptide proton resonances in a different way. It is clear from these ^{1}H NMR titrations that both metals do not fold the peptide into the same conformation.

The lanthanum titration (Figure 4) produced a shifting of most of the peptide resonance lines. The methyl group of *N*-Ac-Asp-103 (2.0 ppm) and some of the methyl groups of ile-110 and Leu-115 (0.8-ppm region) appear the least affected by the presence of the metal. This is expected for free rotating methyl groups located along long aliphatic side chains or at the extremities of the peptide. However, large shifts are observed in the aspartic acid and asparagine β-CH_2 region (2.5–2.9 ppm), residues which are involved in metal ligation. Similar events occur in the β-CH_2 (2.0 ppm) and γ-CH_2 (2.28 ppm) resonance regions of Glu-113 and Glu-114 (–Z).

A remarkable shift of the α-proton resonances of Gly-108 (3.90 ppm) is observed. This result suggests that one of the protons is magnetically shielded upon peptide folding. The doublet centered at 3.8 ppm is shifted to 3.5 ppm in the La^{3+}-saturated spectrum. Another interesting metal-induced shift is that of the methyl resonances of Ala-106 and Ala-112 into different environments. The initial doublet at 1.39 ppm gives rise to two doublets centered at 1.47 and 1.33 ppm, respectively.

In Figure 5, the lutetium titration of AcSTnC(103–115)-amide reveals less extensive shifting of resonances. For example, the Gly-108 α-carbon proton quartet at 3.9 ppm only shifts apart by 0.146 ppm [$(\delta_A - \delta_B)_{initial}$ = 0.109 ppm; $(\delta_A - \delta_B)_{final}$ = 0.255 ppm] as compared to 0.395 ppm [$(\delta_A - \delta_B)_{initial}$ = 0.109 ppm; $(\delta_A - \delta_B)_{final}$ = 0.504 ppm] for the La^{3+} titration. A similar observation can be made for the alanine methyl protons (1.4 ppm), where both doublets remain poorly resolved in the presence of lutetium. The β-CH_2 envelope of aspartic acid-103 (+X), -107 (+Z), and -111 (–X) and asparagine-105

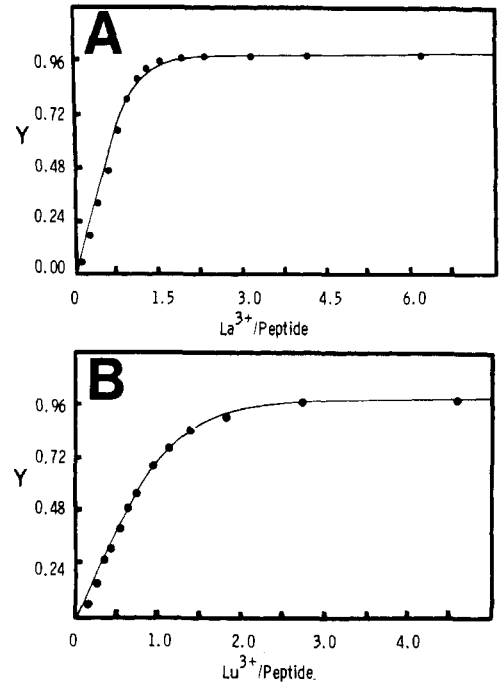

FIGURE 6: Lanthanide titration plots of AcSTnC(103–115)amide. (A) Lanthanum titration; (B) lutetium titration. The observed chemical-shift ratio (Y) was plotted as a function of metal added to the peptide solution. The quantity Y is described under Experimental Procedures.

(+Y) located in the 2.5–2.8-ppm region remains sensitive to the addition of the metal as do the β-CH_2 (2.0 ppm) and γ-CH_2 (2.28 ppm) regions of Glu-113 and -114 (–Z).

Lanthanide Binding Constants. As described under Experimental Procedures, the quantity Y was evaluated for several resonances during each addition of a metal solution. The Y values were determined from the spectral lines of *N*-Ac-Asp-103, the methyl groups of Ala-106 and Ala-112, the α-CH_2 protons of Gly-108, and the β-CH_2 group and aromatic (2,6) ring protons of Tyr-109. Figure 6 shows plots obtained for a typical lanthanum (panel A) and lutetium (panel B) titration of the peptide as a function of the metal to peptide ratio. In the case of both metals, the maximum shift observed for all resonances monitored appears to be reached near a metal:peptide ratio of 1:1, suggesting a 1:1 stoichiometry for the metal/peptide complex. The calculated La^{3+} binding constant was equal to 1.1×10^5 M^{-1} (average of three titrations). The peptide showed a lesser ability to bind lutetium ($K_{Lu^{3+}}$ of 1.3×10^4 M^{-1}; average of two titrations).

Discussion

The metal-induced folding of calcium binding proteins has been mostly described in macroscopic terms using circular dichroism, magnetic resonance techniques, and fluorescence spectroscopy. Actual site-specific folding events and geometric constraints placed on the metal coordination sphere are major issues in our quest to understand the action of such calcium-modulated proteins. We therefore synthesized a 13-residue fragment representing the calcium binding region of site 3 of rabbit skeletal troponin C (residues 103–115; Figure 2) and made use of high-field ^{1}H NMR methods to analyze the binding events during a metal titration of this simpler system.

The diamagnetic lanthanides La^{3+} ($4f^0$) and Lu^{3+} ($4f^{14}$) were used in this study because of their strong binding to this synthetic fragment. Lutetium and lanthanum were selected over other lanthanides because, as in the case of calcium, their observable effect on the ^{1}H NMR spectrum of AcSTnC-

(103–115)amide is free of paramagnetically induced shifting and broadening of resonances. The spectrum perturbations are solely the result of a restricted geometry adopted by the peptide upon metal binding.

Because there is more than one aspartic acid, glutamic acid, and alanine in the sequence (Figure 2), the assignment of their proton resonances is a more difficult task. The metal-free spectrum of AcSTnC(103–115)amide is shown in Figure 3, and the overlapping methyl resonances of the two alanines (1.4 ppm) exemplify the problems in assigning the resonances of a small peptide lacking geometric constraints. The coupling patterns of various regions of the spectrum were analyzed by selectively irradiating each of the spectral lines. The observed connectivities between regions in addition with the recently published resonance pattern of individual amino acids in synthetic tetrapeptides (Bundi & Wurthrich, 1979) permitted the assignment of most resonances. Thus, each amino acid in the peptide sequence can be partly characterized by one or several resonances (Table II). In the absence of metal, the peptide possesses little structure as the resonances of Tyr-109 [β-CH_2, 3.0 ppm; ring (2,6), 7.1 ppm; ring (3,5), 6.8 ppm], *N*-acetyl-Asp-103 (2.0 ppm), and Ala-106 and -112 (β-CH_2, 1.4 ppm) resemble, in terms of line position and pattern, the resonances observed in model compounds.

We have previously demonstrated by circular dichroism that 12- and 21-residue-long synthetic fragments of this site bind calcium poorly [(for AcSTnC(103–114), $K_{Ca^{2+}} = 2 \times 10^2$ M^{-1}; for AcSTnC(103–123), $K_{Ca^{2+}} = 3.1 \times 10^2$ M^{-1}] (Reid et al., 1980, 1981). However, lanthanides are known to bind tighter to calcium binding proteins. In the case of rabbit skeletal troponin C (Wang et al., 1981), terbium(III) binding constants of 5.2×10^8 and 9.7×10^6 M^{-1} and europium(III) binding constants of 4.7×10^9 and 5.3×10^7 M^{-1} have been calculated for the calcium high (2×10^7 M^{-1}) and low (5×10^5 M^{-1}) affinity sites (Potter & Gergely, 1975). From these results, we expected lanthanides to bind strongly to our peptide.

Addition of either La^{3+} (Figure 4) or Lu^{3+} (Figure 5) demonstrated that the peptide adopts a different conformation upon metal binding, with lanthanum producing larger chemical-shift differences than lutetium. It should be noted at this point that La^{3+} (ionic radius, 1.03 Å) has a larger ionic radius than Lu^{3+} (ionic radius, 0.86 Å) or calcium (ionic radius, 1.00 Å). We rationalize a lowering of the metal binding constant to the fact that the peptide geometry around the metal is less compact. This can be visualized by the fact that in the case of lutetium, the peptide ligands interact with a metal which is 20% smaller than lanthanum. This situation will bring the four negatively charged side chains (Asp-103, -107, and -111 and Glu-114) closer together and thus cause ligand repulsion. If the peptide was to assume the same conformation as in the presence of lanthanum, then the bonds between ligands and metal would be 0.17 Å longer, a factor that could well reduce the stability of the metal/peptide complex. Metal binding constants were obtained by a least-squares fitting of typical plots like the ones shown in Figure 6. These results suggested a metal to peptide stoichiometry of 1:1. The calculated metal association constants were respectively equal to 1.1×10^5 M^{-1} for La^{3+} and 1.3×10^4 M^{-1} for Lu^{3+}. Furthermore, the qualitative behavior of the line widths of the AB pattern of the glycine α-protons centered at 3.90 ppm is an indication of the off rate (k_{off}) for the bound metal ion. These resonances initially broaden and then sharpen during the lanthanum titration as compared to a simple shifting pattern observed in the case of lutetium addition (Figures 4 and 5). This suggests that the off rate for the bound La^{3+} is lower than that for Lu^{3+}, which correlates with the larger binding constant. The binding order observed also agrees with the lanthanide affinities measured on native troponin C (Wang et al., 1981) where Eu(III) (ionic radius, 0.95 Å) binds tighter than Tb(III) (ionic radius, 0.92 Å) to both the high- and low-affinity sites.

A look at isolated resonances of the peptide yields information about the actual folding of the peptide. Position 6 of the calcium binding loop (Figure 2), for example, is highly conserved throughout the sequence alignment of calcium binding proteins (Barker et al., 1978; Reid & Hodges, 1980). Glycine normally occupies this position. A notable exception is a serine substitution observed for the alkali light chain of rabbit skeletal muscle myosin, a known non calcium binding EF hand. Proline or lysine substitutions at this position in intestine calcium binding proteins (Hoffman et al., 1979; Fullmer & Wasserman, 1981) and in brain S-100a,b (Isobe & Okuyama, 1981) are followed by an inserted residue and lead to a distorted metal binding region (Szebenyi et al., 1981) that retains its calcium binding ability. Our ^1H NMR results suggest that Gly-108 adopts a rigid environment even in the apopeptide form. This conclusion was drawn from the observation that its α-carbon protons appear as an AB quartet centered at 3.90 ppm. The addition of either lanthanum or lutetium promotes the shielding of one of the α-carbon protons as observed from the upfield shift of two resonances (3.85 and 3.78 ppm) of the quartet (Figures 4 and 5). The shielding effect is larger in the presence of La^{3+} than in the case of Lu^{3+} addition (upfield shift for La^{3+}, 0.315 ppm; upfield shift for Lu^{3+}, 0.095 ppm). This upfield shift can be rationalized by looking at the stereoprojection of this synthetic fragment presented in Figure 7. This projection was constructed by using the peptide backbone coordinates of carp parvalbumin (Kretsinger & Nockolds, 1973) to which our peptide side-chain sequence was substituted. It points out that the glycine α-carbon protons are in close proximity to the aromatic side chain of Tyr-109 and may be shielded through a ring-current effect. Another possibility is the proximity of one of the protons to the carbonyl group of Tyr-109 involved in the coordination sphere. The carbonyl group generates a shielding cone perpendicular to its C–O double-bond plane. The lack of evolutionary divergence at this position of the loop is probably linked to the presence of the α-carbon near various ligands involved in metal chelation. These ligands require some flexibility in order to properly fold around the metal. One can appreciate this fact by considering a substitution to a bulkier side chain. The presence of such a side chain could well hinder the binding of the Asp-103 side chain or Tyr-109 carbonyl group to the metal (Figure 7). Also, the protein backbone chain undergoes a large change in direction in this part of the EF loop (Kretsinger, 1980).

Another site of interest is the –Y position occupied by tyrosine-109. This site represents the least conserved position of the calcium binding loop in terms of amino acid substitutions (Gariépy, 1983). However, the carbonyl group at this position represents the –Y ligand, and the side chain, because of its location in the loop, is thought to play a role in the metal dehydration process (Reid & Hodges, 1980). In view of its hydrophobic side chain, tyrosine-109 appears to be a residue of choice in helping to dehydrate the metal inner-sphere complex. The ^1H NMR spectrum of the peptide aromatic region pointed out the upfield movement of the ring 2,6-proton resonances during addition of lanthanides and in particular lanthanum. A crossover of the ring proton resonances had been observed in earlier studies on both synthetic (Gariépy et al., 1982) and natural fragments of this site (Birnbaum &

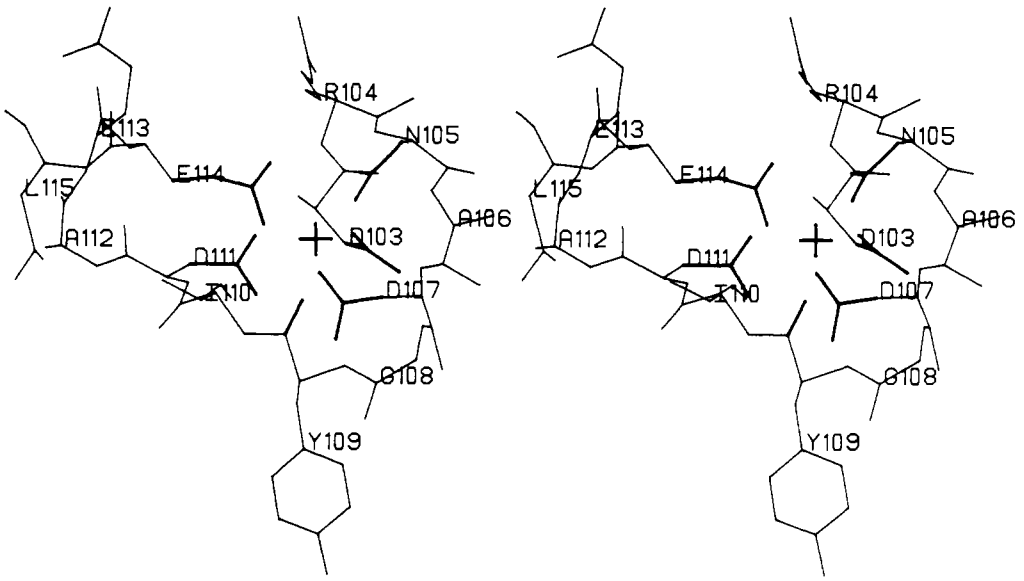

FIGURE 7: Stereoprojection of rabbit skeletal troponin C region 103–115. This representation was constructed by using the crystal coordinates of carp parvalbumin for the metal binding loop of the CD hand (residues 51–63) (Kretsinger & Nockolds, 1973). The original set of coordinates from the peptide backbone was retained, but the rabbit skeletal troponin C side chains of residues 103–115 were substituted for the parvalbumin side chains. The orientation of the side chains along their respective C^{α}–C^{β} bond was maintained. This drawing can more easily be viewed in stereo with a stereoscope obtained from Hubbard Scientific Co., Northbrook, IL.

Sykes, 1978). In all cases, the 2,6-proton lines appear upfield shifted while the 3,5-proton resonances were not significantly altered by the presence of calcium. These observations have led to the idea that geometric constraints were placed on the ring, in the metal-bound conformation. It was further thought that the shielding effect on the tyrosine 2,6 ring protons was a reflection of the change of environment of the side chain. Our present lanthanide results point out that the metal-bound environment of the tyrosine side chain remains closely associated with the loop (upfield shift of the 2,6 ring proton resonances). Furthermore, the addition of the relaxation probe gadolinium, to the metal-bound or metal-free peptide, produces a rapid broadening of the meta-protons' doublet as compared to the ortho-protons' doublet and does indicate that these protons are closer to the metal than the ortho protons.[2] One possible position for the ring can be obtained by a simple rotation of the side chain along its C^{α}–C^{β} bond toward the carbonyl group of Asp-107 or Gly-108. These latter groups will provide a shielding mechanism for the meta protons which remain closer to the metal than the ortho ones.

The reason for wanting to investigate the tyrosine environment in our fragment comes from the observation that it is also exposed to the solvent in calcium-saturated troponin C. For example, the tyrosine rings of troponin C have been labeled by lactoperoxidase iodination (Seamon et al., 1977) and by tetranitromethane (McCubbin & Kay, 1975) in the presence or absence of calcium. Similarly, ^{1}H NMR CIDNP experiments demonstrated clearly that although the exposure of the rings to the excited flavin dye is reduced in the presence of calcium, the effect is quite apparent (Hincke et al., 1981b). If one considers the dimensions of the dye and its hydrophobic nature, one can conclude that the tyrosine ring remains exposed to the solvent, in the metal-saturated protein. The troponin C model proposed by Kretsinger & Barry (1975) illustrates this point. The tyrosine ring exposure is thus similar to the one observed for our peptide. Looking at Figure 7, one realizes that if the tyrosine side chain gets partly immobilized in between the peptide backbone of Gly-108 and Asp-107, it might well explain the shielded environment of one of the α-carbon protons of glycine-108.

Finally, the involvement of Asp-103 as the +X coordinate was confirmed here since the *N*-acetyl resonance (2.0 ppm) of this group titrates to a new position in the presence of these metals. As expected, the interaction appears weaker in the case of lutetium.

In conclusion, this work has indicated that a 13-residue peptide representing a calcium binding region of site 3 of rabbit skeletal troponin C can be used in concert with ^{1}H NMR to answer questions relating to metal binding. It was found that an increase in metal charge was an important factor in the metal binding properties of our peptide since lanthanides have a higher affinity to the loop than calcium (Reid et al., 1980). Also, it was found that lanthanides differing in ionic radius will induce a different peptide conformation. The observed lanthanide binding constants were calculated to be equal to 1.1×10^5 M^{-1} for La^{3+} and 1.3×10^4 M^{-1} for Lu^{3+}. It thus appears that the metal radii will influence the binding properties of the calcium binding loop. Work in our laboratory is now in progress to reconstruct the three-dimensional geometry of the site by using the broadening effect of the isotropic metal gadolinium on selected proton resonances of the peptide.

Acknowledgments

We thank M. Nattriss for performing the amino acid analyses of the samples used in this study. We also acknowledge the help of Masao Fujinaga with regard to the use of the MMS-X computer graphic system.

Registry No. AcSTnC(103–115)amide, 84648-71-5; calcium, 7440-70-2; lanthanum, 7439-91-0; lutetium, 7439-94-3.

References

Barker, W. C., Ketcham, L. K., & Dayhoff, M. O. (1978) in *Atlas of Protein Sequence and Structure* (Dayhoff, M., Ed.) Vol. 5, Suppl. 3, p 273, The National Biomedical Research Foundation, Silver Spring, MD.

Birnbaum, E. R., & Sykes, B. D. (1978) *Biochemistry 17*, 4965–4971.

Bundi, A., & Wurthrich, K. (1979) *Biopolymers 18*, 285–297.

[2] J. Gariépy, B. D. Sykes, and R. S. Hodges, unpublished experiments.

Burtnick, L. D., McCubbin, W. D., & Kay, C. M. (1975) *Can. J. Biochem. 53*, 15–20.
Collins, J. H., Greaser, M. L., Potter, J. D., & Horn, M. J. (1977) *J. Biol. Chem. 252*, 6356–6362.
Crouch, T. H., & Klee, C. B. (1980) *Biochemistry 19*, 3692–3698.
Evans, J. S., Levine, B. A., Leavis, P. C., Gergely, J., Grabarek, Z., & Drabikowski, W. (1980) *Biochim. Biophys. Acta 623*, 10–20.
Fullmer, C. S., & Wasserman, R. H. (1981) *J. Biol. Chem. 256*, 5669–5674.
Gariépy, J. (1983) Ph.D. Thesis, University of Alberta, Edmonton, Alberta, Canada.
Gariépy, J., Sykes, B. D., Reid, R. E., & Hodges, R. S. (1982) *Biochemistry 21*, 1506–1512.
Grabarek, Z., Drabikowski, W., Leavis, P. C., Rosenfeld, S. S., & Gergely, J. (1981) *J. Biol. Chem. 256*, 13121–13127.
Hincke, M. T., McCubbin, W. D., & Kay, C. M. (1978) *Can. J. Biochem. 56*, 384–395.
Hincke, M. T., Sykes, B. D., & Kay, C. M. (1981a) *Biochemistry 20*, 3286–3294.
Hincke, M. T., Sykes, B. D., & Kay, C. M. (1981b) *Biochemistry 20*, 4185–4193.
Hoffman, T., Kawakami, M., Hitchman, A. J., Harrison, J. E., & Dorrington, K. J. (1979) *Can. J. Biochem. 57*, 737–748.
Isobe, T., & Okuyama, T. (1981) *Eur. J. Biochem. 116*, 79–86.
Kanellis, P., Yang, J., Cheung, H., & Lenkinski, R. E. (1983) *Biochim. Biophys. Acta* (in press).
Klee, C. B. (1977) *Biochemistry 16*, 1017–1024.
Kretsinger, R. H. (1976) *Annu. Rev. Biochem. 45*, 239–266.
Kretsinger, R. H. (1977) in *Calcium-Binding Proteins and Calcium Function* (Wasserman, R. H., Corradino, R. A., Carafoli, E., Kretsinger, R. H., MacLennan, D. H., & Siegel, F. L., Eds.) p 63, Elsevier/North-Holland, New York.
Kretsinger, R. H. (1979) *Adv. Cyclic Nucleotide Res. 11*, 1–26.
Kretsinger, R. H. (1980) *CRC Crit. Rev. Biochem. 8*, 119–174.
Kretsinger, R. H., & Nockolds, C. E. (1973) *J. Biol. Chem. 248*, 3313–3326.
Kretsinger, R. H., & Barry, C. D. (1975) *Biochim. Biophys. Acta 405*, 40–52.
LaPorte, D. C., Wierman, B. M., & Storm, D. R. (1980) *Biochemistry 19*, 3814–3819.
Leavis, P. C., & Kraft, E. L. (1978) *Arch. Biochem. Biophys. 186*, 411–415.
Leavis, P. C., Rosenfeld, S. S., Gergely, J., Grabarek, Z., & Drabikowski, W. (1978) *J. Biol. Chem. 253*, 5452–5459.
Lee, L., & Sykes, B. D. (1980a) *Biochemistry 19*, 3208–3214.
Lee, L., & Sykes, B. D. (1980b) *Biophys. J. 32*, 193–210.
Lee, L., & Sykes, B. D. (1981) *Biochemistry 20*, 1156–1162.
Lee, L., & Sykes, B. D. (1982) in *Biochemical Structure Determination by NMR* (Bothner-By, A. A., Glickson, J. D., & Sykes, B. D., Eds.) pp 169–188, Marcel Dekker, New York.
Lee, L., Sykes, B. D., & Birnbaum, E. R. (1979) *FEBS Lett. 98*, 169–172.
Lenkinski, R. E., Yang, J., Cheung, H. C., Stephens, R. L., & Kanellis, P. (1983) *Biochim. Biophys. Acta* (in press).
Levine, B. A., Mercola, D., Coffman, D., & Thornton, J. M. (1977) *J. Mol. Biol. 115*, 743–760.
Martin, R. B., & Richardson, F. S. (1979) *Q. Rev. Biophys. 12*, 181–209.
McCubbin, W. D., & Kay, C. M. (1975) *FEBS Lett. 55*, 183–187.
Mrakovcic, A., Oda, S., & Reisler, E. (1979) *Biochemistry 18*, 5960–5965.
Nagy, B., & Gergely, J. (1979) *J. Biol. Chem. 254*, 12732–12737.
Nagy, B., Potter, J. D., & Gergely, J. (1978) *J. Biol. Chem. 253*, 5971–5974.
Nieboer, E. (1975) *Struct. Bonding (Berlin) 22*, 1–47.
Potter, J. D., & Gergely, J. (1975) *J. Biol. Chem. 250*, 4628–4633.
Reid, R. E., & Hodges, R. S. (1980) *J. Theor. Biol. 84*, 401–444.
Reid, R. E., Clare, D. M., & Hodges, R. S. (1980) *J. Biol. Chem. 255*, 3642–3646.
Reid, R. E., Gariépy, J., Saund, A. K., & Hodges, R. S. (1981) *J. Biol. Chem. 256*, 2742–2751.
Reuben, J. (1977) in *Calcium Binding Proteins and Calcium Function* (Wasserman, R. H., Corradino, R. A., Carafoli, E., Kretsinger, R. H., MacLennan, D. H., & Siegel, F. L., Eds.) p 21, Elsevier/North-Holland, New York.
Seamon, K. B. (1979) *Biochem. Biophys. Res. Commun. 86*, 1256–1265.
Seamon, K. B. (1980) *Biochemistry 19*, 207–215.
Seamon, K. B., Hartshore, D. J., & Bothner-By, A. A. (1977) *Biochemistry 16*, 4039–4046.
Shannon, R. D. (1976) *Acta Crystallogr., Sect. A A32*, 751–767.
Szebenyi, D. M. E., Obendorf, S. K., & Moffat, K. (1981) *Nature (London) 294*, 327–332.
Vogt, H.-P., Strassburger, W., Wollmer, A., Fleischhauer, J., Bullard, B., & Mercola, D. (1979) *J. Theor. Biol. 76*, 297–310.
Walsh, M., Stevens, F. C., Oikawa, K., & Kay, C. M. (1978) *Biochemistry 17*, 3924–3930.
Walsh, M., Stevens, F. C., Oikawa, K., & Kay, C. M. (1979) *Can. J. Biochem. 57*, 267–278.
Wang, C.-L. A., Leavis, P. C., Horrocks, W. DeW., Jr., & Gergely, J. (1981) *Biochemistry 20*, 2439–2444.
Wolff, D. J., Poirier, P. G., Brostrom, C. O., & Brostrom, M. A. (1977) *J. Biol. Chem. 252*, 4108–4117.